DOI: 10.1093/brain/awg203 Advanced Access publication June 23, 2003 *Brain* (2003), **126,** 2093–2107

Occipito-temporal connections in the human brain

Marco Catani,[1] Derek K. Jones,[2] Rosario Donato[3] and Dominic H. ffytche[1]

[1]*Institute of Psychiatry, London, UK,* [2]*Section of Tissue Biophysics and Biomimetics, Laboratory of Integrative and Medical Biophysics, National Institute of Child Health and Human Development, National Institutes of Health, Bethesda, MD, USA and* [3]*Section of Anatomy, Department of Experimental Medicine and Biochemical Sciences, University of Perugia, Perugia, Italy*

Correspondence to: Marco Catani or Dominic ffytche, Institute of Psychiatry, De Crespigny Park, London SE5 8AF, UK
E-mail: m.catani@iop.kcl.ac.uk or d.ffytche@iop.kcl.ac.uk

Summary

Diffusion tensor MRI (DT-MRI) provides information about the structural organization and orientation of white matter fibres and, through the technique of 'tractography', reveals the trajectories of cerebral white matter tracts. We used tractography in the living human brain to address the disputed issue of the nature of occipital and temporal connections. Classical anatomical studies described direct fibre connections between occipital and anterior temporal cortex in a bundle labelled the inferior longitudinal fasciculus (ILF). However, their presence has been challenged by more recent evidence suggesting that connections between the two regions are entirely indirect, conveyed by the occipito-temporal projection system—a chain of U-shaped association fibres. DT-MRI data were collected from 11 right-handed healthy subjects (mean age 33.3 ± 4.7 years). Each data set was co-registered with a standard MRI brain template, and a group-averaged DT-MRI data set was created. 'Virtual' *in vivo* dissection of occipito-temporal connections was performed in the group-averaged data. Further detailed virtual dissection was performed on the single brain data sets. Our results suggest that in addition to the indirect connections of the occipito-temporal projection system: (i) a major associative connection between the occipital and anterior temporal lobe is provided by a fibre bundle whose origin, course and termination are consistent with classical descriptions of the ILF in man and with monkey visual anatomy; (ii) the tractography-defined ILF is structurally distinct from fibres of the optic radiation and from U-shaped fibres connecting adjacent gyri; (iii) it arises in extrastriate visual 'association' areas; and (iv) it projects to lateral and medial anterior temporal regions. While the function of the direct ILF pathway is unclear, it appears to mediate the fast transfer of visual signals to anterior temporal regions and neuromodulatory back-projections from the amygdala to early visual areas. Future tractography studies of patients with occipito-temporal disconnection syndromes may help define the functional roles of the direct and indirect occipito-temporal pathways.

Keywords: tractography; inferior longitudinal fasciculus; occipito-temporal connections

Abbreviations: DT-MRI = diffusion tensor MRI; ILF = inferior longitudinal fasciculus; LGN = lateral geniculate nucleus; ROI = region of interest

Introduction

The inferior longitudinal fasciculus (ILF), a white matter associative tract connecting the occipital and temporal lobes, was first described in 1822 by the German neuroanatomist K. F. Burdach (Polyak, 1957). Since its initial description, the ILF has been the subject of several studies with contrasting conclusions. Whilst some authors consider the ILF to be the major occipito-temporal associative tract (Dejerine, 1895; Crosby *et al*., 1962; Gloor, 1997), others deny its existence (Putnam, 1926; Polyak, 1957; Tusa and Ungerleider, 1985). For example, using blunt dissection in human and monkey brains, Tusa and Ungerleider (1985) were unable to demonstrate long associative fibres interconnecting occipital and anterior temporal lobes distinct from those of the optic radiation. They concluded that 'Burdach's ILF is nothing more than a portion of the geniculo-striate pathway that has been mislabelled'. Furthermore, their autoradiographic experiments indicated that 'the pathway from the occipital to the temporal cortex in monkeys consists of a series of U fibres that course beneath the cortical mantle to connect adjacent regions in striate, pre-striate, and inferior temporal

cortex'. They suggested that, like the monkey, the occipital and anterior temporal lobes in man are connected indirectly through a series of U fibres passing visual signals from one area to the next in a series of hierarchical steps. They also proposed that the term ILF be replaced with the term 'occipito-temporal projection system' (Tusa and Ungerleider, 1985).

While the anatomical evidence for an ILF is disputed, over the last century, several neuropsychological syndromes have been attributed to a disruption of specific fibre connections between visual and temporal cortex. These syndromes include: associative visual agnosia (for a review see Jankowiak and Albert, 1994), prosopagnosia (Benson *et al*., 1974; Meadows, 1974), visual amnesia (a deficit of registering novel visual experiences in short-term memory with the preserved ability to register novel, non-visual experiences; Ross, 1980) and visual hypo-emotionality (a deficit of visually evoked emotions with preserved emotional responses to non-visual stimuli; Bauer, 1982; Habib, 1986; Sierra *et al*., 2002). (For an extensive review of visual disconnection syndromes see Geschwind, 1965*a*,*b*; Girkin and Miller, 2001.) Common to them all is the idea that the transection of fibres transferring signals from 'visual' areas to 'emotional' and 'memory' areas results in a visually specific semantic, emotional or memory deficit. Advances in non-invasive functional imaging and the doctrine of functional specialization have led to a re-interpretation of some of these syndromes in terms of damage to specialized cortical modules, e.g. prosopagnosia with lesions of face-specialized cortex (Sergent *et al*., 1992). However, there remain some for which the deficit seems better explained by a disconnection than a loss of specialized cortex (e.g. visual amnesia and visual hypo-emotionality). Often these syndromes follow widespread occipito-temporal lesions that extend into underlying white matter and, consequently, could equally relate to Tusa and Ungerleider's occipito-temporal projection system as to a direct ILF connection. However, in some rare examples, the disconnection follows lesions that spare the indirect occipito-temporal projection system. For example, in one of the visual amnesia cases described by Ross (1980), occipito-temporal cortex and U-shaped fibres were largely unaffected, the critical lesion being a small infarct, posterior and inferior to the occipital horn of the left lateral ventricle, the classical location of the ILF.

Although the neuropsychological evidence for a direct (as opposed to indirect) connection between occipital and anterior temporal lobes is limited, another line of evidence suggests that such a pathway is present in the human brain. Wilson *et al*. (1983) found some cells in the parahippocampal gyrus that responded to visual stimuli at a latency of 47 ms, only 2 ms after cells in the occipital lobe. Other cells in the same region responded with a latency of 200 ms. The 2 ms latency difference is consistent with a direct pathway from occipital to parahippocampal cortices, but is too short to reflect a multisynaptic pathway through several visual areas. The latency evidence is thus suggestive of two pathways connecting occipital and anterior temporal regions: a direct short-latency pathway and an indirect long-latency pathway.

The neuropsychological and neurophysiological evidence thus raises the question of whether Tusa and Ungerleider's dismissal of the ILF was premature. Might the classical anatomists have been correct in describing a direct connection between occipital and anterior temporal regions? A recent development in neuroimaging, tractography, seemed a promising tool with which to explore this issue. MR tractography (Basser, 1998; Jones *et al*., 1998, 1999; Mori *et al*., 1998, 1999; Conturo *et al*., 1999; Basser *et al*., 2000; Parker *et al*., 2002; Poupon *et al*., 2000) is based on diffusion tensor MRI (DT-MRI) (Basser *et al*., 1994) and allows white matter neuroanatomy to be studied non-invasively in the living human brain.

The aim of tractography is to reconstruct the 3D trajectories of white matter tracts, by following a continuous path of greatest diffusivity (i.e. least hindrance to diffusion) through the brain from one region to another. We recently used virtual *in vivo* interactive dissection (VIVID) tractography to elucidate the 3D morphometry of the major white matter fasciculi within the living human brain (Catani *et al*., 2002). Our results demonstrate that virtual tract maps obtained using VIVID are faithful to the classical descriptions of white matter tracts that have been documented previously by more invasive means. Furthermore, in a previous study, we demonstrated the possibility of performing tractography on a population-averaged diffusion tensor data set (Jones *et al*., 2002*a*), and showed a 'summary' tractography result for a group of subjects, i.e. a map that summarizes the trajectories of the major white matter pathways, as seen by DT-MRI, within a group of subjects, emphasizing anatomical features common to each subject of the group. Given these previous results, tractography seemed a promising tool with which to explore the neuroanatomy of occipito-temporal connections in the human brain with the specific aim of establishing support for the presence or absence of an inferior longitudinal fasciculus and, if present, of describing its detailed neuroanatomy as revealed by tractography.

Method

Data acquisition

Eleven, right-handed, healthy male volunteers (mean age 33.3 $\pm$ 4.7 years) were enrolled in this study according to the following criteria: (i) age range between 25 and 40 years; (ii) no previous history of head injury; (iii) no history of neurological or psychiatric disorders; (iv) no current psychotropic medication; and (v) diabetes and chronic hypertension excluded. The study was approved by the Institute of Psychiatry research ethics committee and all the subjects gave informed consent. DT-MRI data were acquired from a 1.5 T GE Signa LX system (General Electric, Milwaukee, WI) with 40 mT/m gradients. The acquisition was gated to the cardiac cycle using a peripheral gating

device placed on the subjects' forefinger. A multislice peripherally gated echo-planar imaging (EPI) acquisition sequence, fully optimized for DT-MRI of white matter, was used, providing isotropic resolution (2.5 mm × 2.5 mm × 2.5 mm) and coverage of the whole head (Jones *et al*., 2002*b*). Sixty contiguous near-axial slice locations with isotropic resolution were acquired for each subject with an echo time of 107 ms and an effective repetition time of 15 R–R intervals. The duration of the diffusion-encoding gradients was 17.3 ms, giving a maximum diffusion weighting of 1300 s/mm^2. The total data acquisition time was ~14 min. Full details of the data acquisition are provided in Jones *et al*. (2002*b*). Following correction for image distortions introduced by the application of the diffusion-encoding gradients, the diffusion tensor was determined in each voxel following the method described by Basser *et al*. (1994). The fractional anisotropy (Basser and Pierpaoli, 1996), a measure that quantifies the degree of tissue ordering within each voxel on a scale from 0 to 1 (with a high value corresponding to structures being highly aligned within the voxel), was computed within each voxel.

Spatial normalization and averaging of diffusion tensor MRI data sets

In order to obtain a group-averaged DT-MRI data set in a standard anatomical reference space, a template DT-MRI data set was generated in a standard anatomical space by co-registering with a T_2-weighted EPI template included as part of the functional imaging analysis software package SPM99 (statistical parametric mapping; Wellcome Department of Cognitive Neurology, Institute of Neurology, London, UK). One subject was identified from the group of 11 subjects, whose age was close to the mean age of the remaining 10 subjects (age of eleventh subject = 33 years, mean age of remaining 10 subjects = 33.3 years), and his data set was used to create the DT-MRI template. The computed T_2-weighted volume data set obtained as part of the diffusion tensor fitting procedure was masked from the background signal using a brain extraction procedure described in Jones *et al*. (2002*a*). The data were then imported into SPM99 and the 'Spatial Normalisation' feature used to co-register this T_2-weighted volume with the T_2-weighted volume template supplied in SPM, using an affine transformation with 12 degrees of freedom (Friston *et al*., 1995*a*,*b*). The affine transformation matrix thus obtained was then applied to the fractional anisotropy volume data set of this subject to create a 'target' fractional anisotropy data template in a standard reference space. Each of the remaining 10 subject's data sets was co-registered (using an affine registration with 12 degrees of freedom) to the target fractional anisotropy volume using the approach described by Alexander *et al*. (2001). This approach employs the AIR (automated image registration) package (Woods *et al*., 1998*a*,*b*) for co-registration, and the computed transformations thus obtained were applied to the DT-MRI volumes using the Preservation of Principal Directions algorithm (Alexander *et al*., 2001), which has been shown to reorient each tensor correctly under non-rigid transformations. The fractional anisotropy volumes (Basser and Pierpaoli, 1996) were used for co-registration. Following co-registration into a common reference space, a mean of the 10 diffusion tensors in each voxel was computed (Jones *et al*., 2002*a*) to produce a mean diffusion tensor volume data set.

Tractography

The software for estimating and reconstructing the trajectories of tracts from DT-MRI data was written in the 'C' programming language. A set of locations for the initiation of the tracking algorithm (referred to here as 'seedpoints') was first selected on the fractional anisotropy images. For each of these seedpoints, the orientation of the diffusion tensor was estimated. The tracking algorithm then moved a distance of 0.5 mm along this direction. The diffusion tensor at this new location was determined from a continuous description of the tensor field (Pajevic *et al*., 2002) and its orientation subsequently estimated. The algorithm then moved a further 0.5 mm along this direction. A pathway was traced out in this manner until the fractional anisotropy of the tensor fell below an arbitrary threshold (set to 0.20 in this case). The procedure was then repeated by tracking in the opposite direction to the first step at the seedpoint, in order to reconstruct the whole tract passing through the seedpoint (Basser *et al*., 2000). A three-dimensional representation of the pathways was then generated by creating a set of polygons with circular cross-section, and fixed radius, to connect up the points, using MATLAB (Catani *et al*., 2002).

Virtual dissection of occipito-temporal connections

To virtually dissect the white matter tracts of the occipital and temporal lobes, a two region of interest (ROI) approach was used, such that only those trajectories passing through both regions were retained for the analysis (Catani *et al*., 2002). The ROIs were selected by using classical neuroanatomical works (Dejerine, 1895; Ludwig and Klingler, 1956), and standard textbooks (Crosby *et al*., 1962; Nieuwenhuys *et al*., 1988) as a reference. Using the methods described below, the following white matter tracts were virtually dissected: (i) the visual pathway from post-chiasmic optic tract to optic radiation (including the temporal loop); (ii) splenial fibres terminating in occipital cortex; (iii) candidate inferior longitudinal fasciculus fibres; and (iv) U-shaped association fibres.

Visual pathway

To dissect the visual pathway, three different ROIs were defined. A central ROI around the lateral geniculate nucleus

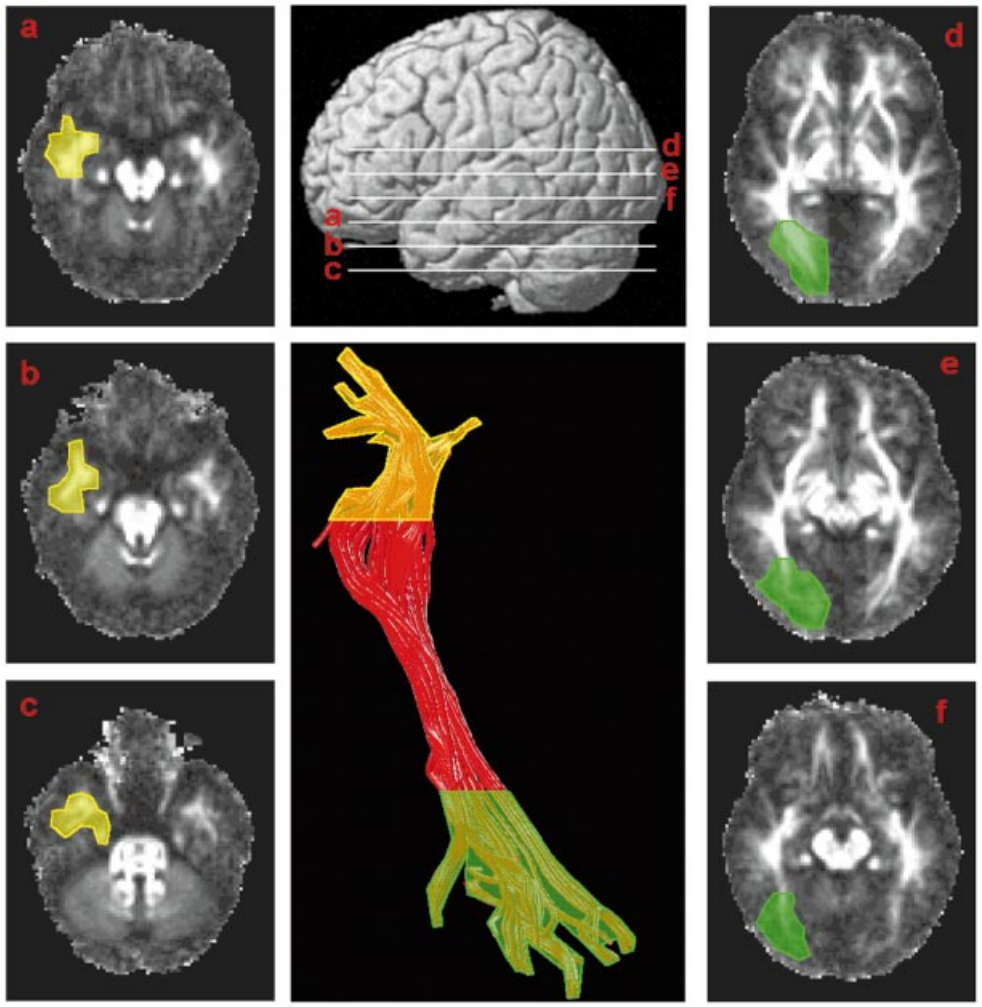

Fig. 1 Location of the occipital and anterior temporal ROIs used to identify long associative occipito-temporal fibres. A series of axial fractional anisotropy slices are shown, with the anterior temporal region coloured in yellow and the occipital region coloured in green. The location of each slice is shown by the corresponding letter in the lateral brain view (middle panel upper row). The middle panel of the bottom row shows the long fibres connecting the two regions coloured red, with the portion lying within the anterior temporal ROI coloured yellow and the occipital ROI coloured green.

(LGN), a second ROI in the white matter of the optic tract and a third ROI in the white matter of the occipital lobe. The first and second regions were used to visualize the fibres of the optic tract and the first and third region to visualize the optic radiations.

Splenial fibres

A two ROI approach was used to dissect the splenial fibres of the corpus callosum connecting the medial cortex of left and right occipital lobes. One region was located in the forceps major of the left hemisphere, and the other in the forceps major of the right hemisphere. The splenial fibres provided a reference point from which to compare the anatomical relationships of the visual pathways and ILF.

ILF

We used a two ROI approach to dissect candidate fibres for the ILF. The first ROI surrounded the white matter of the anterior temporal lobe (see Fig. 1 for ROIs). The posterior border of this region was defined by the anterior extent of the fibres of the temporal loop and the inferior extent of the fibres of the inferior fronto-occipital fasciculus to avoid inclusion of these bundles. The second ROI was defined around the white matter of the occipital lobe.

U-shaped fibres

To dissect U-shaped fibres, a single ROI was placed along the lateral surface of the temporal lobe in a single brain data set. We found that by restricting the seedpoints to the lateral-most

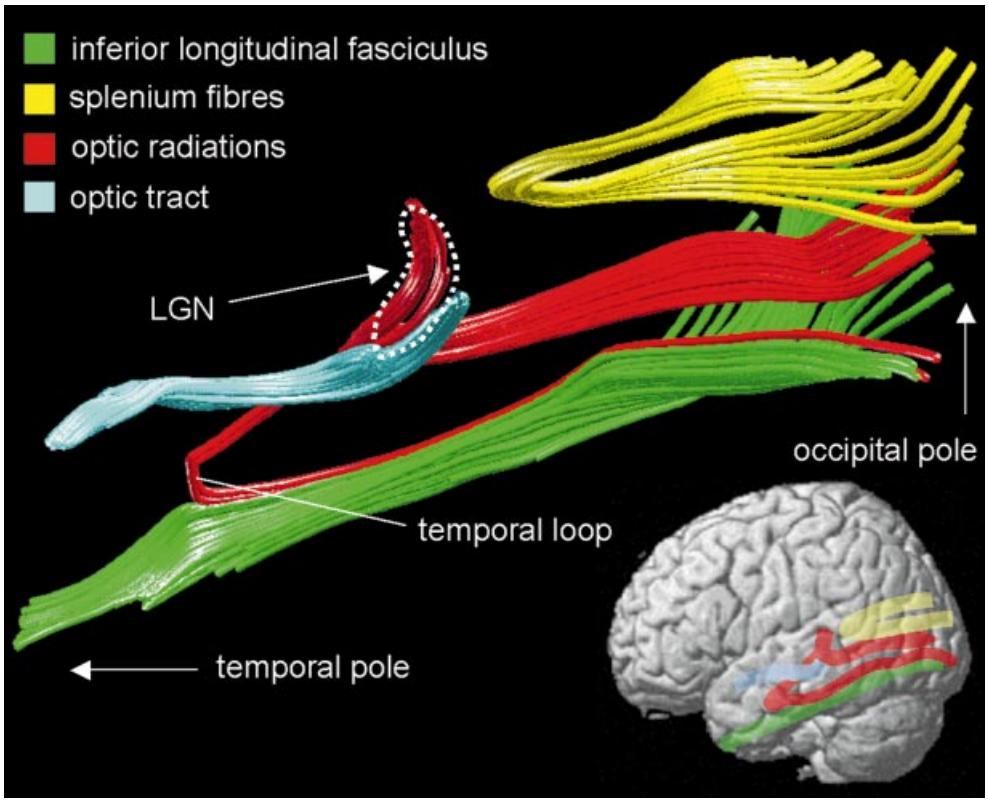

Fig. 2 Virtual *in vivo* dissection of the ILF and visual pathway of the right hemisphere (medial view) in the average brain data set. Splenial fibres connecting medial occipital regions are also shown. See text for explanation.

white matter, the tractography algorithm only reconstructed U-shaped fibres. A single brain was used, as individual variations in gyrification mean that U-shaped fibres from each subject are not superimposed in Talairach space and, although present in the individual brains, do not appear in the average DT-MRI data set (Jones *et al*., 2002*a*).

The tractography-defined trajectories of white matter were displayed as 3D objects, intersecting horizontal slices through the fractional anisotropy volumes, allowing us to examine their origin, course and termination with reference to recognizable anatomical structures. This procedure was used for both average brain and single brain data sets. The average brain was used to examine anatomical features common to all the subjects in the group. The Talairach coordinates of the origin and termination branches of the ILF were used to assign functional labels by comparison with previous functional imaging studies. Since anatomically variable features such as the distal portions of ILF branches are lost in the averaging method (see Discussion), the exact cortical destinations of the fibres are only approximate, being inferred from the position and orientation of the average branch end points. Furthermore, since diffusion anisotropy in the cortical region is very low (Pierpaoli *et al*., 1996), it is impossible to track reliably into the cortex itself. Single brain data sets were used to examine the detailed anatomy of ILF branches and of U-shaped fibres.

Results

Our tractography dissections provide support for a fibre bundle connecting occipital and anterior temporal regions, distinct from the optic radiation and from U-shaped association fibres. Figs 2–4 show the visual pathway, splenial and occipito-temporal fibre bundles in the average data set, displayed in different colours. Below, we describe the detailed neuroanatomy of each virtually dissected fibre bundle.

Visual pathway

As the optic nerve fibres leave the chiasm (not shown in the figures) and enter the optic tract, they describe an 'italic s' shape (Fig. 3) and terminate in the antero-ventral portion of the LGN. With the image resolution employed in this study, the voxel-averaged anisotropy of grey matter is low and, hence, in our data sets, it is not possible to visualize grey matter nuclei directly. However, by following the distribution of terminating fibres, it is possible to define approximately the shape of the area corresponding to the LGN. This bean-shaped space has been defined by the dotted line in Figs 2–4. The fibres of the optic tract enter the LGN antero-ventrally, whilst the fibres of the optic radiation leave the LGN from its posterior dorso-lateral surface. The fibres of the geniculo-calcarine tract divide into two bundles: a ventral temporal

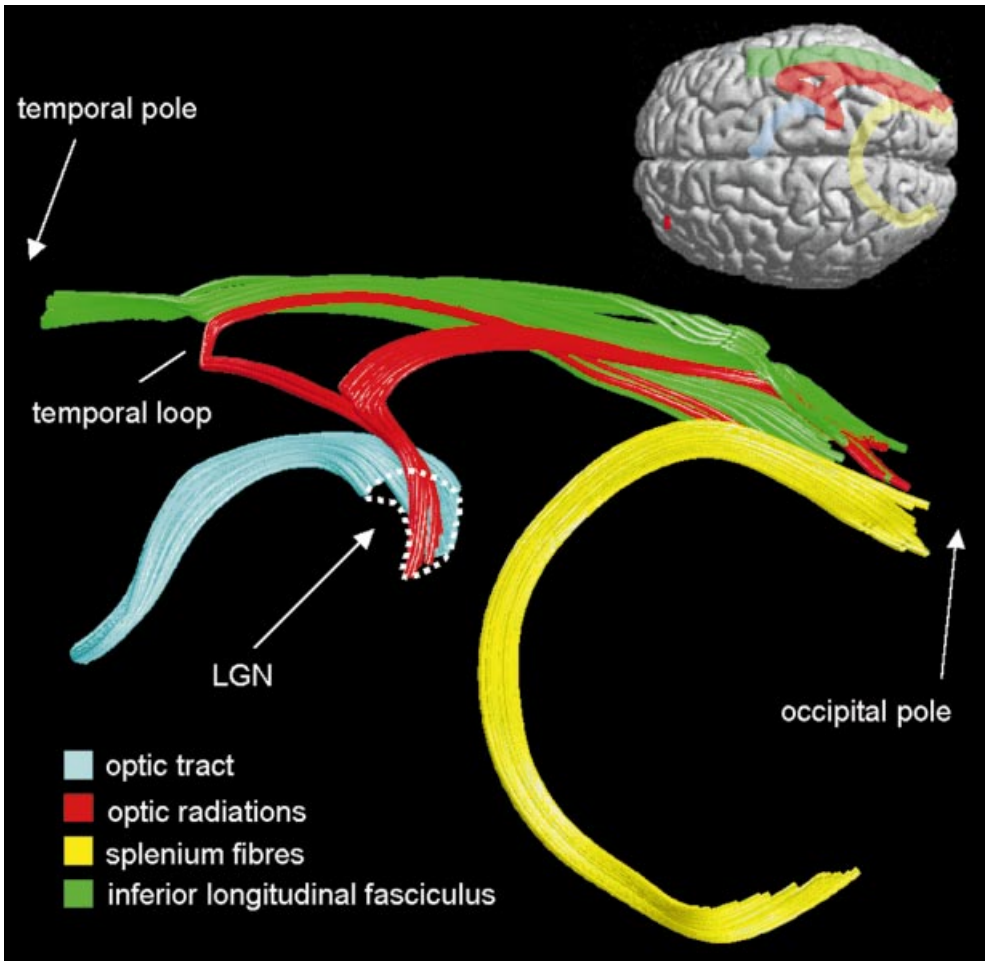

Fig. 3 Virtual *in vivo* dissection of the ILF and visual pathway of the right hemisphere (top view) in the average brain data set. See text for explanation.

loop and a dorsal optic radiation. Although these two bundles originate from the same region of the LGN, their origin is slightly different, the fibres of the dorsal optic radiation arising dorsally to those of the temporal loop (Fig. 4). The small temporal loop bundle passes below the dorsal optic radiation fibres and projects forward and laterally towards the temporal pole. After a short run, the temporal loop describes a sharp arc around the temporal horn of the lateral ventricle and continues backward towards the occipital pole where it terminates in the lower calcarine lip. As the fibres of the dorsal optic radiations leave the LGN, they assemble into a thick, compact lamina and, after a short lateral course, bend posteriorly towards the occipital pole, terminating in the upper calcarine lip.

ILF

We were able to identify a fibre bundle distinct from that of the temporal loop of the optic radiation, connecting posterior occipital with anterior temporal regions (Figs 2–4). The origin, course and termination of this bundle are shown in Figs 5–8, with the Talairach coordinates for the branches given in Table 1. The terms origin and termination are used for convenience only, as the DT-MRI method is blind to whether the fibres represent feed-forward or feed-backward connections. The occipital branches of the ILF arise in extrastriate cortical regions on the dorso-lateral surface of the occipital lobe, ventro-medially from the posterior lingual gyrus and fusiform gyri and dorso-medially from the cuneus (Fig. 5). The cuneal branch is less apparent in the average brain, but a bifurcation of the dorsal stem into medial and lateral branches is clearly visible. The branches run forward, parallel to the fibres of the splenium and optic radiation and, at the level of the posterior horn of the lateral ventricle, gather in a single bundle (Fig. 6). In the anterior temporal lobe, the branches pass to the superior, middle and inferior temporal gyri on the lateral surface of the temporal lobe and medially to the uncus/parahippocampal gyrus close to the amygdala and hippocampus (Figs 5–7). No long fibres were identified with an origin in the calcarine fissure. An important observation was that the ILF was distinct from the U-shaped fibres connecting adjacent gyri and forming the occipito-temporal projection system, i.e. the chain of indirect connections between occipital and temporal lobes (Fig. 8).

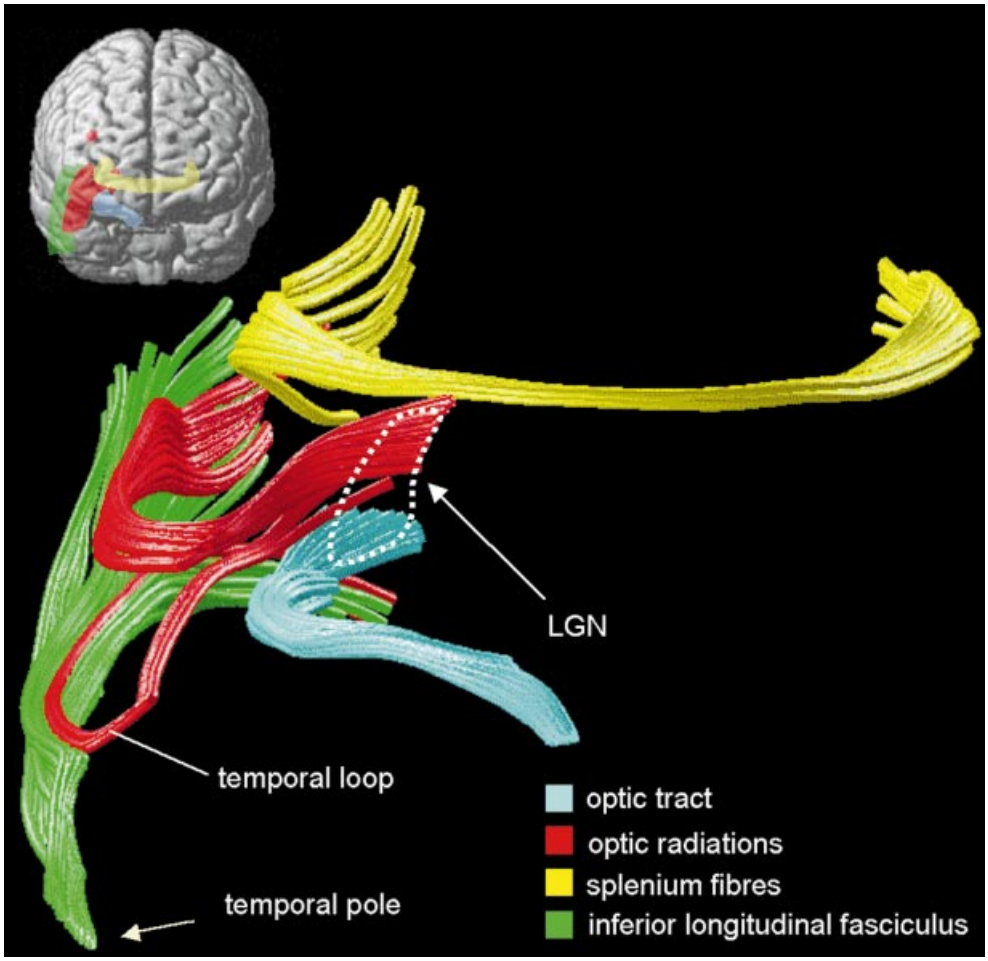

Fig. 4 Virtual *in vivo* dissection of the ILF and visual pathway of the right hemisphere (anterior view) in the average brain data set. See text for explanation.

Discussion

We used tractography to visualize occipito-temporal connections within the living human brain. Previous studies have questioned the existence of a fibre bundle connecting occipital and anterior temporal lobes directly, arguing that such fibres represent an anatomical artefact, the mislabelled ventral portion of the optic radiation, and that occipital-temporal connections are indirect. Our tractography results are consistent with an occipito-temporal pathway distinct from that of the optic radiations and from the U-shaped projection system. Below we argue that the close correspondence between the tractography-defined anatomy in our study, the anatomy of the monkey visual system and classical anatomical descriptions is strongly suggestive of the existence of an ILF in man.

Historical context

The origin, course and termination of our tractography-defined optic radiation match previous descriptions from classical post-mortem neuroanatomical works (Dejerine, 1895; Ludwig and Klingler, 1956) and standard textbooks (Crosby *et al*., 1962; Nieuwenhuys *et al*., 1988; Gloor, 1997). For example, the tractography-defined details of the termination of the optic tract fibres in the antero-ventral aspect of the LGN were consistent with previous well-documented descriptions (Polyak, 1957). We have also been able to reproduce the origin of the fibres of the optic radiation and to distinguish the ventral temporal and dorsal optic radiations with their terminations in the superior and inferior banks of the calcarine cortex—the cortical representations of the inferior and superior quadrants of the contralateral visual field (Inouye, 1909; Holmes, 1945; Horton and Hoyt, 1991*a*). The optic radiations were first described in 1856 by Gratiolet, but it was Flechsig who, 40 years later in 1896, first called attention to the peculiar course of the ventral fibres of the optic radiation. He named the sharp turn made by the ventral optic radiation the 'temporal knee', 'temporal detour' or 'temporal loop'. The ventral pathway was studied subsequently by several authors, and its discovery was attributed erroneously by some investigators to A. Meyer and to H. Cushing. For this reason, it has been suggested the term 'Meyer's loop' be replaced with 'Flechsig–Meyer's loop' (for a historical review see Polyak, 1957).

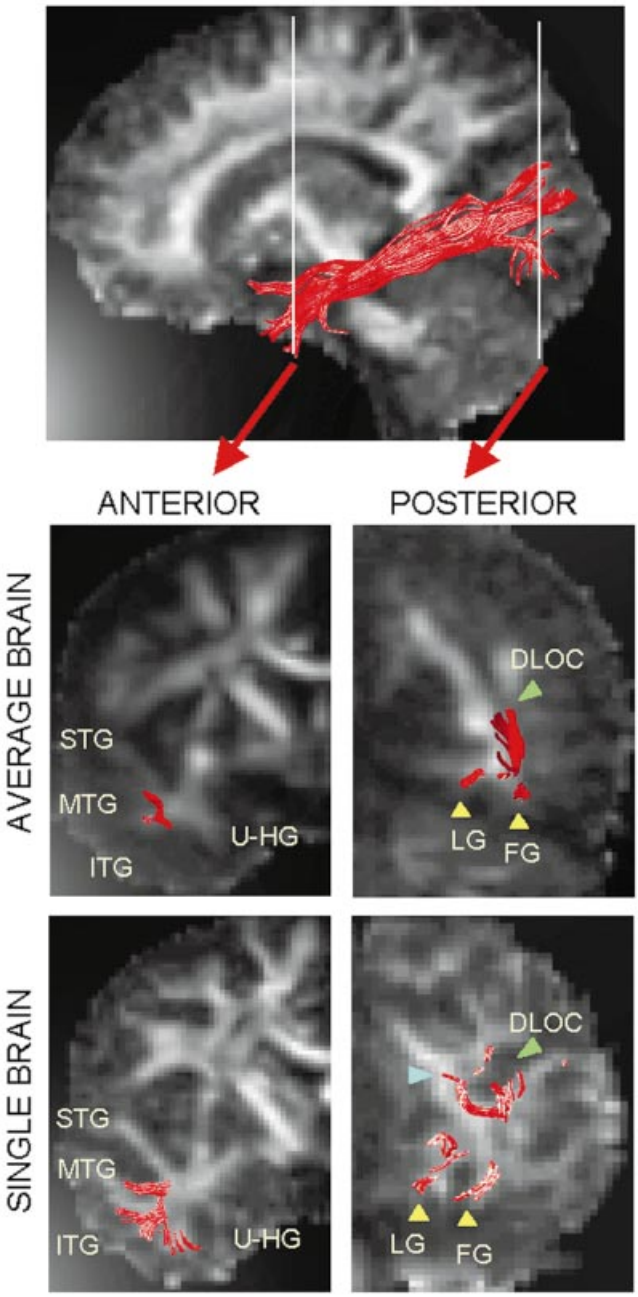

Fig. 5 Terminal branches of the ILF in the temporal (left column) and occipital (right column) ROIs in the average and single brains. The fibres are co-registered on coronal slices of the average DT-MRI brain (the slice locations are indicated in the sagittal section at the top of the figure). The top pair of images relates to the average brain, the bottom pair to the single subject brain. In the occipital lobe, the ILF originates from the dorso-lateral occipital cortex (green arrowhead), cuneus (blue arrowhead), posterior lingual and fusiform gyri (yellow arrowhead). The terminal branches are not as well defined in the average as in the single brain, although it is possible to recognize a similar distribution of the fibres. STG = superior temporal gyrus; MTG = middle temporal gyrus; ITG = inferior temporal gyrus; U-HG = uncus/parahippocampal gyrus; LG = lingual gyrus; FG = fusiform gyrus; DLOC = dorso-lateral occipital cortex.

Using *in vivo* tractography, we demonstrated long associative fibres connecting occipital and anterior temporal lobes in human brains. The tractography-defined fibres are entirely consistent with previous anatomical descriptions of the ILF (Dejerine, 1895; Ludwig and Klingler, 1956; Crosby *et al*., 1962; Nieuwenhuys *et al*., 1988). First, in both the classical anatomical descriptions and our tractography results, fibres originate in extrastriate visual 'association areas' of the occipital lobe, sparing the primary visual cortex. Crosby *et al*. (1962) describe three branches of origin: a lingual branch, a lateral occipital branch and a cuneal branch, all of which were identified in our tractography study. Secondly, our DT-MRI data show the ILF to be distinct from the fibres of the Fleschig–Meyer loop. At the occipital horn of the lateral ventricle, the ILF fibres run laterally to the optic radiation and callosal (tapetal) fibres, the three bundles corresponding to the external, intermediate and internal sagittal strata of Sachs (Dejerine, 1895; Crosby *et al*., 1962; Nieuwenhuys *et al*., 1988). Thirdly, in the anterior temporal lobe, both the classical anatomical and tractography-defined fibres terminate in lateral and medial temporal areas. Crosby *et al*. (1962) describe lateral temporal branches to superior, middle and inferior temporal gyri and medial branches to the parahippocampal gyrus, the same distribution found in our average and single subject DT-MRI data sets. The correspondence of our tractography-defined ILF origin, course and termination with classical anatomical descriptions cannot be accounted for by *a priori* constraints imposed by our ROI method, and provides strong supportive evidence for the existence of an ILF in man.

Comparison with non-human primate anatomy

The neuroanatomy of the human visual system is less well characterized than that of non-human primates (Crick and Jones, 1993). The macaque visual system consists of multiple map-like areas, each specialized for different visual attributes, connected by feed-forward and feed-back pathways (Zeki and Shipp, 1988; Felleman and Van Essen, 1991). These areas form an approximate hierarchy based on the pattern of connectivity (an area is lower in the hierarchy from that to which it sends feed-forward connections and higher in the hierarchy than that from which it receives feed-forward connections). Taken together, the connected areas form extended pathways, one passing to the temporal lobe specialized for the processing of visual objects (the ventral stream) and the other to the parietal lobe specialized for the processing of spatial location (the dorsal stream) (Mishkin *et al*., 1983). The primary visual receiving area, the striate cortex (V1), is situated in monkey and man at the occipital pole extending along the medial surface of the occipital lobe and, to a varying degree in man (Brindley, 1972) and more consistently in the monkey, to the lateral occipital surface. Beyond V1, further consistencies between the monkey and human visual system have been found in the specializations of cortical visual areas for different visual attributes, e.g.

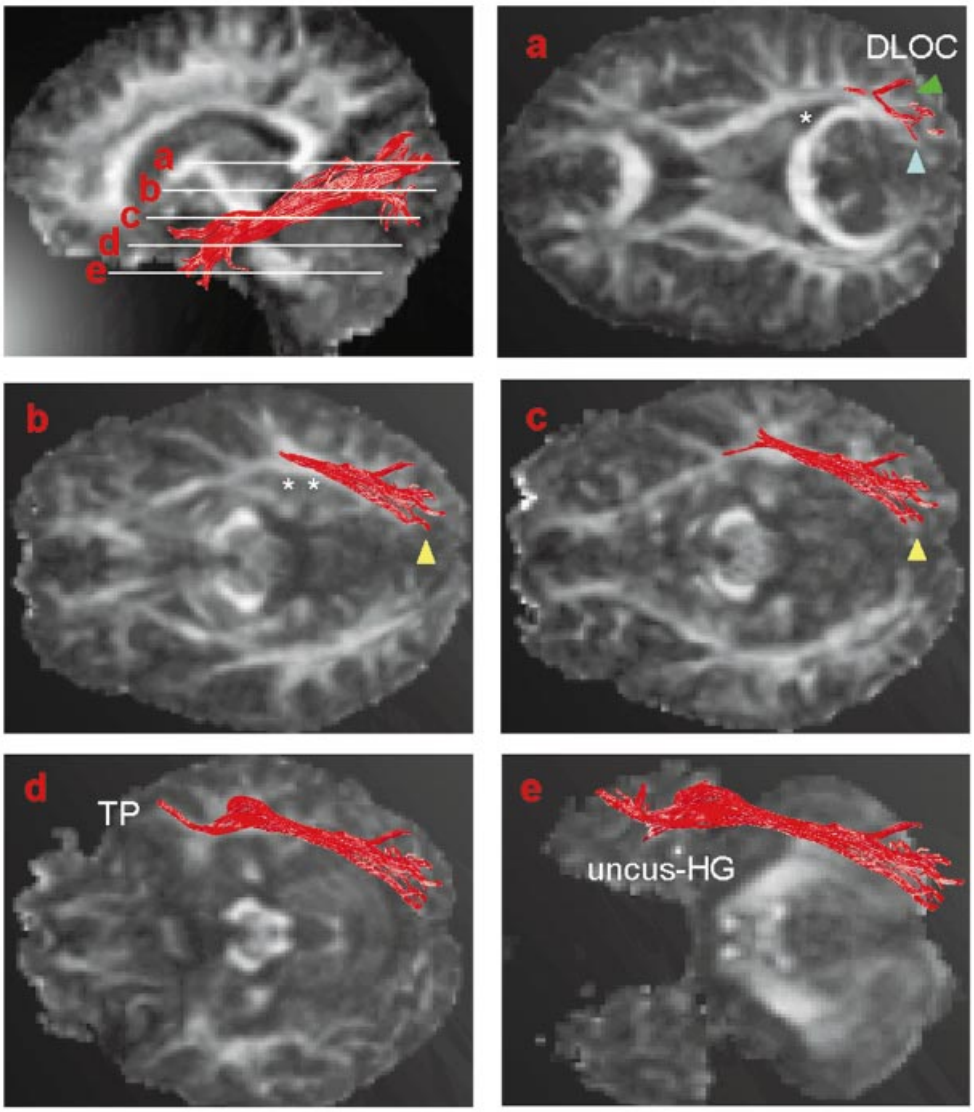

Fig. 6 The fibres of the ILF in a single brain have been co-registered with axial fractional anisotropy slices (the slice locations are indicated in the sagittal section at the top left of the figure). (**a–c**) In the occipital lobe, the ILF originates from the lateral occipital cortex (green arrowhead), cuneus (blue arrowhead), posterior lingual and fusiform gyri (yellow arrowhead). The fibres run anteriorly and, as they reach the posterior horn of the lateral ventricle (*), are gathered in a single bundle. The ILF continues along the major axis of the temporal lobe lateral to the lateral ventricle (**). (**d** and **e**) In the anterior temporal lobe, the ILF projects laterally to superior, middle and inferior temporal gyri, and medially to the parahippocampal gyrus and amygdala. DLOC = dorso-lateral occipital cortex; HG = parahippocampal gyrus; TP = temporal pole.

colour (V4) and motion (V5) (Zeki *et al*., 1991). Our results suggest further that these inter-species consistencies extend to white matter tracts, as we found striking similarities between the occipito-temporal connections identified by DT-MRI in man and those described in the monkey. Like Tusa and Ungerleider (1985) and Kuypers *et al*. (1965), the former using autoradiographic injections and the latter using lesions of pre-striate cortex, we found no evidence for direct connections between the striate cortex and the anterior temporal lobe, although the possibility that a few fibres connect these regions cannot be excluded due to the limited resolution of DT-MRI. In the monkey studies, the main projection to the ventro-lateral surface of the temporal lobe is from V4, an area that also projects to the parahippocampal gyrus (Martin-Elkins and Horel, 1992). Furthermore, the amygdala sends back-projections to V4 and V2 (Amaral and Price, 1984; Iwai and Yukie, 1987). Our method is blind to whether individual branches of the ILF are feed-forward, feed-back or mixed; however, we found a pattern of connectivity in our tractography-defined ILF consistent with the connectivity predicted by monkey studies. The ventral fusiform branch of the ILF falls within the coordinates of

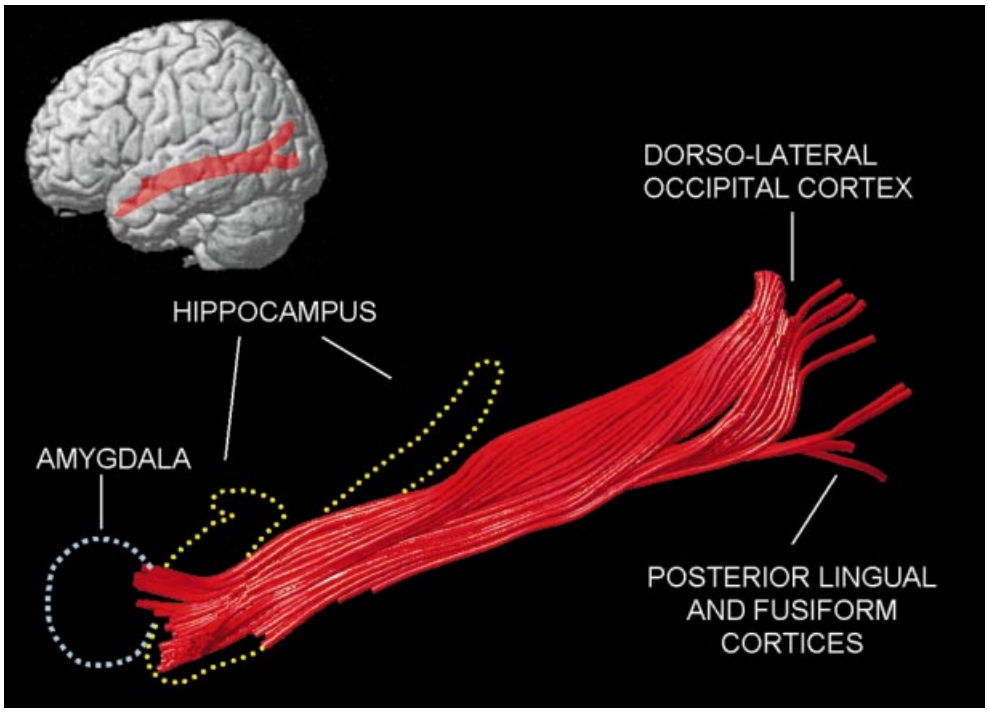

Fig. 7 Reconstruction of the ILF in the average DT-MRI data set. The long fibres originate from extrastriate areas of the occipital lobe and terminate in lateral temporal cortex and medial temporal cortex in the region of the amygdala and parahippocampal gyrus.

human V4 (McKeefry and Zeki, 1997) and connects to lateral temporal and medial temporal parahippocampal regions, as does V4 in the monkey. Although the prediction of the monkey studies would be a series of branches along the ventro-lateral aspect of the temporal lobe, our method ignores such branches, restricting fibres to those connecting our *a priori* ROIs. It would seem likely, therefore, that, in addition to the lateral temporal branches identified anteriorly, further lateral branches arise along the entire extent of the ILF.

With regards to the branch of the tractography-defined ILF in the region of the amygdala, monkey studies predict feed-back connections from amygdala to V2 and V4 (Iwai and Yukie, 1987; sparse back-projections to V5 and V1 were also identified, but the limited number of fibres involved makes it unlikely that they would be detectable using DT-MRI). In man, V2 is located on the lingual gyrus, cuneus and lateral surface of the occipital lobe (Horton and Hoyt, 1991*b*; Sereno *et al*., 1995), showing a perfect correspondence with the locations of the tractography-defined occipital ILF branches. Like the feed-forward projections from monkey V4 described above, back-projections from the amygdala pass to lateral temporal cortical areas that would not have been identified using our ROI method. A connection between V4 and the medial temporal lobe has already been described above and is consistent with a back-projection to V4 from the amygdala. Based on the monkey data, we would predict the V4 branch of the ILF to carry feed-forward connections to the parahippocampal gyrus and feed-back connections from the amygdala.

The ILF as an anatomical artefact?

The existence of an ILF has been disputed by some researchers who have argued that it represents the ventral portion of the geniculostriate pathway (Putnam, 1926; Polyak, 1957; Tusa and Ungerleider, 1985). Tusa and Ungerleider (1985), using blunt dissection in human and monkey brains, found: '….a single fibre bundle from occipital to temporal cortex…..which when viewed in coronal sections corresponds to the ventral portion of the external sagittal stratum in the occipital lobe and to the entire external sagittal stratum in the temporal lobe…..'. They conclude that: ' ….the external sagittal stratum has been shown repeatedly to contain the geniculostriate pathway. Our data are therefore consistent with previous anatomical work suggesting that Burdach's ILF is nothing more than a portion of the geniculostriate pathway that has been mislabelled. Specifically, this fibre bundle corresponds to the ventral portion of the geniculostriate pathway in the occipital lobe and to Meyer's loop in the temporal lobe…...'. We argue that the location of a set of fibres in the external sagittal stratum need not imply that they belong to the optic radiations. Our results agree with Tusa and Ungerleider in apportioning occipito-temporal fibres to the external sagittal stratum. Where they differ is in our virtual dissection of a fibre bundle distinct from that of the optic radiation. The bundle is unlikely to represent an anatomical anomaly as it is derived from an average DT-MRI data set and therefore reflects anatomical features consistent across subjects. While post-mortem dissection, such as performed by

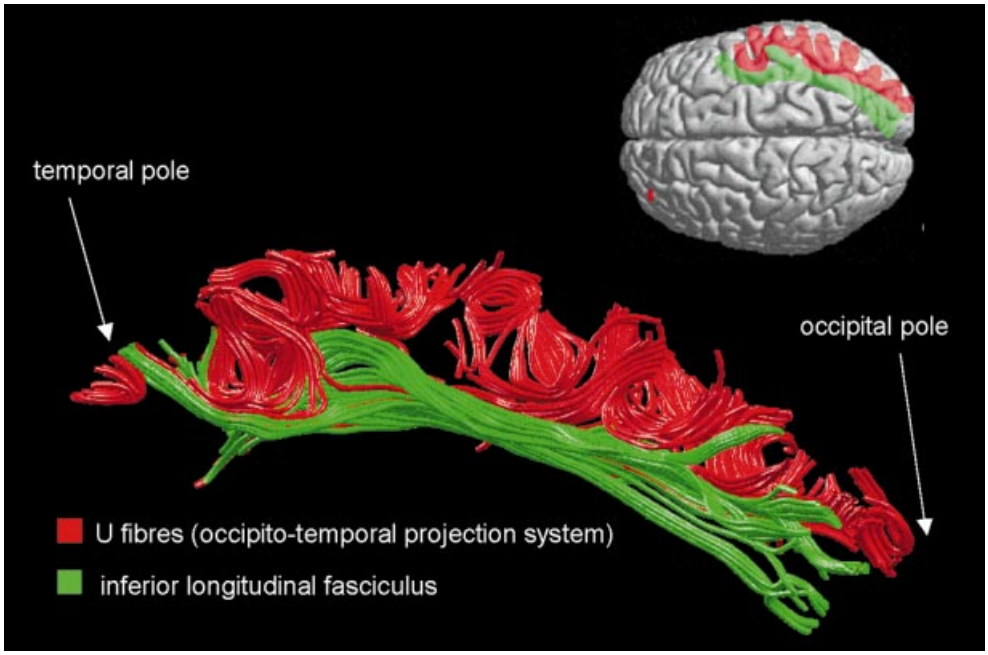

Fig. 8 The ILF (green) and U-shaped fibres (red) of the right hemisphere in a single brain data set. U-shaped fibres are located laterally to the ILF and connect the adjacent gyri of the lateral occipito-temporal cortices to form the occipito-temporal projection system.

Table 1. *Talairach coordinates for the occipito-temporal terminations of the right inferior longitudinal fasciculus*

Areas	Talairach coordinates		
	x	*y*	*z*
Dorso-lateral occipital cortex	16 to 45	–73 to –99	6 to 18
Fusiform/lingual gyri	12 to 42	–63 to –100	–6 to –15
Anterior lateral temporal cortex	43 to 58	5 to 20	–25 to –35
Uncus/hippocampal gyrus	15 to 31	3 to –10	–25 to –35

Tusa and Ungerleider, must remain the definitive standard against which 'virtual' tractography is compared (see below), the fact that, for much of their course, the tractography-defined ILF and the Flechsig–Meyer loop run adjacent to one another would make their dissection in post-mortem brains a particularly difficult task. We would argue that the ILF and optic radiations are easy to confuse but, nevertheless, represent distinct pathways.

Methodological issues

While post-mortem and autoradiographic techniques can trace white matter tracts directly, DT-MRI tractography reconstructs virtual white matter pathways by following pathways of high diffusivity. Consequently, as discussed by other authors (Pierpaoli *et al*., 2001), DT-MRI tractography can, at best, only suggest the presence of white matter pathways that may or may not correspond to true anatomical connections. This aspect of the technique is especially relevant to situations where *a priori* knowledge of white matter neuroanatomy is limited or there are conflicting results. Although DT-MRI previously has produced results that are strikingly similar to post-mortem anatomical studies (Catani *et al*., 2002), all DT-MRI tractography results should be considered as preliminary since, to date, no studies have validated *in vivo* tractography with post-mortem tracing methods. The fact that our dissections were 'virtual' raises the question of whether or not the direct occipito-temporal connections we described are themselves artefactual. However, we do not feel this to be the case. Our ROI method was not tightly constrained *a priori* to be consistent with the classical anatomical or monkey literature, and yet the reconstructed trajectories still closely matched those of the early anatomical descriptions (Dejerine, 1895; Crosby *et al*., 1962; Gloor, 1997). Particularly striking was the fact that we did not artefactually reconstruct any fibre connections to V1

or the anterior temporal pole, which is in accord with both classical anatomical and the monkey literature.

A limitation of tractography is the incomplete representation of fibre bundles. For example, we have already noted that our ILF description excludes branches passing to the lateral temporal lobe. By using a two ROI approach, we display only fibres connecting our two *a priori* regions. The exclusion of the lateral temporal cortex from our ROI was reasonable given that the primary aim of the study was to establish the presence or absence of direct connections between occipital and anterior temporal regions. A further consideration is that, in the study reported here, we used a novel 'average' DT-MRI method which has not been validated extensively, although we have shown in a previous study that anatomically plausible descriptions of white matter fasciculi can be identified (Jones *et al*., 2002*b*). In that study, DT-MRI tractography identified centrally located fasciculi, referred to as the 'stems' by earlier workers (Makris *et al*., 1997), which were consistent between the mean and individual data sets and with previous anatomical studies, suggesting that the method produces anatomically valid results. While the advantage of the averaging method is that anatomy common to all subjects is highlighted, thus identifying the most salient anatomical features, its disadvantage is that it is blind to features with a high degree of variability (e.g. U-shaped fibres, terminal branches of tracts or anatomical features in small structures). The mean tractography results are less representative of the individual data sets in anatomically variable regions than in anatomically invariant regions (Jones *et al*., 2002*a*). Our inability to follow terminal branches in the average brain means that we are only able to infer their final cortical destinations from the location and orientation of the average tract end points. However, the inferred destinations are entirely consistent with the terminal fibres identified in our single brain tractography dissections, giving us confidence in their validity.

Recall that the white matter trajectories were reconstructed iteratively by stepping a small distance parallel to the estimate of fibre orientation at a point. The fibre orientation at the new point subsequently was estimated and the stepping procedure repeated. It has been shown that the uncertainty in fibre orientation is spatially inhomogenous throughout the brain and, even within white matter, varies considerably from point to point (Jones, 2003). Consequently, the 'reliability' of the reconstructions of trajectories (formed from successive estimates of fibre orientation) passing through different parts of the white matter will be variable. The tractography algorithm used in the present study, however, did not incorporate this information and, as such, all reconstructions were deemed equally likely. Quantification of the uncertainty in fibre orientation is indeed possible (Jones, 2003), and this information potentially could be incorporated into tractography algorithms to assign 'confidence' to a tract. However, additional scan time is necessary to acquire this information (at least twice the scan times used here). The present study was a *post hoc* analysis of data acquired for a previous study (Jones *et al*., 2002*a*) during which the additional scanning necessary for obtaining information on the uncertainty in fibre orientation was not performed. Studies collecting sufficient data and development of algorithms that will incorporate this information are currently underway.

Functional significance of the ILF and its associated clinical syndromes

The correspondence of classical anatomical descriptions, the known connections of the monkey visual system and the anatomy of our tractography-defined pathway provides convincing evidence for the existence of an ILF in man. The implication is that, in addition to the serial, hierarchical pathway from occipital to anterior temporal regions through U-shaped fibre connections, signals pass directly to the parahippocampal gyrus and lateral temporal lobe from V4 and return directly from the amygdala to V4 and V2. The direct feed-forward connection from V4 to the parahippocampal gyrus provides an explanation for the short-latency parahippocampal single-cell responses in man described by Wilson (1983). In that study, the onset latency of some parahippocampal gyrus cells differed from those in the occipital cortex by 2 ms, a difference too small to be caused by multisynaptic transmission through the U-shaped fibre occipito-temporal projection system. In fact, other cells were found in the same region with latencies of 200 ms, consistent with multistage hierarchical transmission. The implication of the latency findings is that there are two pathways by which signals reach the parahippocampal gyrus, an indirect long-latency pathway and a direct short-latency pathway. We would argue that the former corresponds to the occipito-temporal projection system and the latter to the ILF. These parallel inputs to the parahippocampal gyrus are analogous to those found in the visual motion system. Here area V5 is activated with a short latency through a direct pathway from the LGN or tecto-pulvinar system and an indirect pathway passing through V1 and V2. The direct LGN or tecto-pulvinar→V5 pathway is associated with a short-latency activation of V5, and the indirect LGN→V1→V2→V5 pathway with a long-latency one (ffytche *et al*., 1995, 1996).

What functions might be served by direct occipito-temporal (and temporo-occipital) pathways and how do they differ from those of the indirect pathway? The question is not easy to answer, as case reports of occipito-temporal disconnection syndromes typically involve lesions of white matter and occipito-temporal cortex, transecting both the indirect occipito-temporal projection system and direct connections in the ILF. One clue may be provided by the patient described by Ross (1980) with a lesion apparently restricted to the direct pathway. The patient was unable to learn novel, non-verbalizable visual stimuli, despite the fact that visual information was able to reach his medial temporal structures through the indirect pathway. Perhaps one function of the direct pathway is to prime medial temporal structures to

facilitate the consolidation of visual memories, although it should be noted that the patient's deficit could also be attributed to a laterality effect (a relative deficiency of the left anterior temporal lobe for spatial compared with verbal memory tasks; see, for example, Kimura, 1963). Whatever the function of the feed-forward direct projection, the direct feed-back projection is easier to interpret. Once the emotional valence of a visual stimulus has been identified, it would seem reasonable to assume that signals will be fed back directly to early visual areas, enhancing the visual processing of emotionally significant stimuli. In support of this view, recent imaging studies have found neuromodulatory effects of the amygdala on extrastriate visual cortex (Morris *et al*., 1998; Pessoa *et al*., 2002), and psychophysical studies have identified an equivalent modulatory effect of emotional content on visual perceptual processing (Anderson and Phelps, 2001). Future tractography studies of patients with occipito-temporal disconnection syndromes may help clarify the functions of the direct ILF pathway and determine how they differ from those of the indirect occipito-temporal projection system.

Conclusion

Our tractography results provide evidence in support of a direct connection from extrastriate occipital cortex to anterior temporal structures in addition to the indirect connections of the occipito-temporal projection system. The fibre bundle is distinct from Fleschig–Meyer's loop of the optic radiation and from U-shaped fibres connecting adjacent gyri, compatible with classical anatomical descriptions of the ILF and studies of the monkey visual system. The tractography results show occipital branches related to areas V2 and V4 and anterior temporal branches related to the lateral temporal cortex, parahippocampal gyrus and amygdala. The connections allow direct, fast access of visual information to anterior temporal structures and from anterior temporal structures to the occipital lobe.

Acknowledgements

We wish to thank Rob Howard for helpful comments. D.H.ff. is a Wellcome Clinician Scientist Fellow.

References

Alexander DC, Pierpaoli C, Basser PJ, Gee JC. Spatial transformations of diffusion tensor magnetic resonance images. IEEE Trans Med Imaging 2001; 20: 1131–9.

Amaral DG, Price JL. Amygdalo-cortical projections in the monkey (Macaca fascicularis). J Comp Neurol 1984; 230: 465–96.

Anderson AK, Phelps EA. Lesions of the human amygdala impair enhanced perception of emotionally salient events. Nature 2001; 411: 305–9.

Basser PJ. Fiber-tractography via diffusion tensor MRI (DT-MRI). In: Proceedings of the ISMRM 6th Annual Meeting, Sydney. 1998. p. 1226.

Basser PJ, Pierpaoli C. Microstructural and physiological features of tissues elucidated by quantitative-diffusion-tensor MRI. J Magn Reson B 1996; 111: 209–19.

Basser PJ, Mattiello J, Le Bihan D. MR diffusion tensor spectroscopy and imaging. Biophys J 1994; 66: 259–67.

Basser PJ, Pajevic S, Pierpaoli C, Duda J, Aldroubi A. In vivo fiber tractography using DT-MRI data. Magn Reson Med 2000; 44: 625–32.

Bauer RM. Visual hypoemotionality as a symptom of visual–limbic disconnection in man. Arch Neurol 1982; 39: 702–8.

Benson DF, Segarra J, Albert ML. Visual agnosia–prosopagnosia. A clinicopathologic correlation. Arch Neurol 1974; 30: 307–10.

Brindley GS. The variability of the human striate cortex. J Physiol 1972; 225: 1P–3P.

Catani M, Howard R, Pajevic S, Jones DK. Virtual in vivo interactive dissection of white matter fasciculi in the human brain. Neuroimage 2002; 17: 77–94.

Conturo TE, Lori NF, Cull TS, Akbudak E, Snyder AZ, Shimony JS, et al. Tracking neuronal fiber pathways in the living human brain. Proc Natl Acad Sci USA 1999; 96: 10422–7.

Crick F, Jones E. Backwardness of human neuroanatomy. Nature 1993; 361: 109–10.

Crosby EC, Humphrey T, Lauer EW. Correlative anatomy of the nervous system. New York: Macmillan; 1962.

Dejerine J. Anatomie des centres nerveux, Vol. 1. Paris: Rueff et Cie; 1895.

Felleman DJ, Van Essen DC. Distributed hierarchical processing in the primate cerebral cortex. Cerebr Cortex 1991; 1: 1–47.

ffytche DH, Guy CN, Zeki S. The parallel visual motion inputs into areas V1 and V5 of human cerebral cortex. Brain 1995; 118: 1375–94.

ffytche DH, Guy CN, Zeki S. Motion specific responses from a blind hemifield. Brain 1996; 119: 1971–82.

Friston KJ, Holmes AP, Worsley KJ, Poline JB, Frith JD, Frackowiak RS. Statistical parametric maps in functional imaging: a general linear approach. Hum Brain Mapp 1995*a*; 2: 189–210.

Friston KJ, Ashburner J, Frith JD, Poline JB, Heather JD, Frackowiak RS. Spatial registration and normalization of images. Hum Brain Mapp 1995*b*; 3: 165–89.

Geschwind N. Disconnexion syndromes in animals and man. Part I. Brain 1965*a*; 88: 237–94.

Geschwind N. Disconnexion syndromes in animals and man. Part II. Brain 1965*b*; 88: 585–644.

Girkin CA, Miller NR. Central disorders of vision in humans. Surv Ophthalmol 2001; 45: 379–405.

Gloor P. The temporal lobe and the limbic system. New York: Oxford University Press; 1997.

Habib M. Visual hypo-emotionality and prosopagnosia associated with right temporal lobe isolation. Neuropsychologia 1986; 24: 577–82.

Holmes G. The Ferrier Lecture: the organization of the visual cortex in man. Proc R Soc (Lond) B 1945; 132: 348–61.

Horton JC, Hoyt WF. The representation of the visual field in human striate cortex: a revision of the classic Holmes map. Arch Ophthalmol 1991*a*; 109: 816–24.

Horton JC, Hoyt WF. Quadrantic visual field defects: a hallmark of lesions in extrastriate (V2/V3) cortex. Brain 1991*b*; 114: 1703–18.

Inouye T. Die Sehstörungen bei Schussverletzungen der kortikalen Sehsphäre: nach Beobachtungen an Verwundeten der letzen japanischen Kriege. Leipzig: W. Engelmann; 1909.

Iwai E, Yukie M. Amygdalofugal and amygdalopetal connections with modality-specific visual cortical areas in macaques (Macaca fuscata, M. mulatta, and M. fascicularis). J Comp Neurol 1987; 261: 362–87.

Jankowiak J, Albert ML. Lesion localization in visual agnosia. In: Kertesz A, editor. Localization and neuroimaging in neuropsychology. San Diego: Academic Press; 1994. p. 429–71.

Jones DK. Determining and visualizing uncertainty in estimates of fiber orientation from diffusion tensor MRI. Magn Reson Med 2003; 49: 7–12.

Jones DK, Simmons A, Williams SCR, Horsfield MA. Non-invasive assessment of structural connectivity in white matter by diffusion tensor MRI. In: Proceedings of the ISMRM 6th Annual Meeting, Sydney. 1998. p. 531.

Jones DK, Simmons A, Williams SCR, Horsfield MA. Non-invasive assessment of axonal fiber connectivity in the human brain via diffusion tensor MRI. Magn Reson Med 1999; 42: 37–41.

Jones DK, Griffin LD, Alexander DC, Catani M, Horsfield MA, Howard R, et al. Spatial normalization and averaging of diffusion tensor MRI data sets. Neuroimage 2002*a*; 17: 592–617.

Jones DK, Williams SCR, Gasston D, Horsfield MA, Simmons A, Howard R. Isotropic resolution diffusion tensor imaging with whole brain acquisition in a clinically acceptable time. Hum Brain Mapp 2002*b*; 15: 216–30.

Kimura D. Right temporal-lobe damage. Arch Neurol 1963; 8: 264–71.

Kuypers HGJM, Szwarcbart MK, Mishkin M, Rosvold HE. Occipitotemporal corticocortical connections in the Rhesus monkey. Exp Neurol 1965; 11: 245–62.

Ludwig E, Klingler J. Atlas cerebri humani. Boston: Little, Brown; 1956.

Makris N, Worth AJ, Sorensen AG, Papadimitriou GM, Wu O, Reese TG, et al. Morphometry of in vivo human white matter association pathways with diffusion-weighted magnetic resonance imaging. Ann Neurol 1997; 42: 951–62.

Martin-Elkins CL, Horel JA. Cortical afferents to behaviorally defined regions of the inferior temporal and parahippocampal gyri as demonstrated by WGA-HRP. J Comp Neurol 1992; 321: 177–92.

McKeefry DJ, Zeki S. The position and topography of the human colour centre as revealed by functional magnetic resonance imaging. Brain 1997; 120: 2229–42.

Meadows JC. The anatomical basis of prosopagnosia. J Neurol Neurosurg Psychiatry 1974; 37: 489–501.

Mishkin M, Ungerleider LG, Macko KA. Object vision and spatial vision: two cortical pathways. Trends Neurosci 1983; 6: 414–7.

Mori S, Crain BJ, van Zijl PC. 3D brain fiber reconstruction from diffusion MRI. Neuroimage 1998; 7: 5710.

Mori S, Crain BJ, Chacko VP, van Zijl PC. Three-dimensional tracking of axonal projections in the brain by magnetic resonance imaging. Ann Neurol 1999; 45: 265–69.

Morris JS, Friston KJ, Büchel C, Frith CD, Young AW, Calder AJ, et al. A neuromodulatory role for the human amygdala in processing emotional facial expressions. Brain 1998; 121: 47–57.

Nieuwenhuys R, Voogd J, van Huijzen C. The human central nervous system. 3rd edn. Berlin: Springer-Verlag; 1988.

Pajevic S, Aldroubi A, Basser PJ. A continuous tensor field approximation of discrete DT-MRI data for extracting microstructural and architectural features of tissue. J Magn Reson 2002; 154: 85–100.

Parker GJM, Stephan KE, Barker GJ, Rowe JB, MacManus DG, Wheeler-Kingshott CAM, et al. Initial demonstration of in vivo tracing of axonal projections in the macaque brain and comparison with the human brain using diffusion tensor imaging and fast marching tractography. Neuroimage 2002; 15: 797–809.

Pessoa L, McKenna M, Gutierrez E, Ungerleider LG. Neural processing of emotional faces requires attention. Proc Natl Acad Sci USA 2002; 99: 11458–63.

Pierpaoli C, Jezzard P, Basser PJ, Barnett AS, Di Chiro G. Diffusion tensor MR imaging of the human brain. Radiology 1996; 201: 637–48.

Pierpaoli C, Barnett A, Pajevic S, Chen R, Penix L, Virta A, et al. Water diffusion changes in wallerian degeneration and their dependence on white matter architecture. Neuroimage 2001; 13: 1174–85.

Polyak S. The vertebrate visual system. Chicago: University of Chicago Press; 1957.

Poupon C, Clark CA, Frouin V, Regis J, Bloch I, Le Bihan D, et al. Regularization of diffusion-based direction maps for the tracking of brain white matter fascicles. Neuroimage 2000; 12: 184–195.

Putnam TJ. Studies on the central visual connections. Arch Neurol Psychiatr 1926; 16: 566–96.

Ross ED. Sensory-specific and fractional disorders of recent memory in man. I. Isolated loss of visual recent memory. Arch Neurol 1980; 37: 193–200.

Sereno MI, Dale AM, Reppas JB, Kwong KK, Belliveau JW, Brady TJ, et al. Borders of multiple visual areas in humans revealed by functional magnetic resonance imaging. Science 1995; 268: 889–93.

Sergent J, Ohta S, MacDonald B. Functional neuroanatomy of face and object processing. Brain 1992; 115: 15–36.

Sierra M, Lopera F, Lambert MV, Phillips ML, David AS.

Separating depersonalisation and derealisation: the relevance of the 'lesion method'. J Neurol Neurosurg Psychiatry 2002; 72: 530–2.

Tusa RJ, Ungerleider LG. The inferior longitudinal fasciculus: a reexamination in humans and monkeys. Ann Neurol 1985; 18: 583–91.

Wilson CL, Babb TL, Halgren E, Crandall PH. Visual receptive fields and response properties of neurons in human temporal lobe and visual pathways. Brain 1983; 106: 473–502.

Woods RP, Grafton ST, Holmes CH, Cherry SR, Mazziotta JC. Automated image registration. I. General methods and intra-subject, intra-modality validation. J Comput Assist Tomogr 1998*a*; 22: 139–52.

Woods RP, Grafton ST, Watson JD, Sicotte NL, Mazziotta JC. Automated image registration.II. Intersubject validation of linear and non-linear models. J Comput Assist Tomogr 1998*b*; 22: 153–65.

Zeki S, Shipp S. The functional logic of cortical connections. Nature 1988; 335: 311–7.

Zeki S, Watson JDG, Lueck CJ, Friston KJ, Kennard C, Frackowiak RSJ. A direct demonstration of functional specialization in human visual cortex. J Neurosci 1991; 11: 641–9.

Received January 17, 2003.
Revised April 17, 2003. Accepted April 21, 2003